Thermotropic Liquid Crystals of Main-Chain Polyesters Having a Mesogenic 4,4′-Biphenyldicarboxylate Unit. 6. Chiral Mesophases of Polyesters with a (*S*)-2-Methylbutylene Spacer

Junji Watanabe,* Manabu Hayashi, Atushi Morita, and Masatoshi Tokita

Department of Polymer Chemistry, Tokyo Institute of Technology, Ookayama, Meguro-ku, Tokyo 152, Japan

Received April 6, 1995; Revised Manuscript Received July 19, 1995[⊗]

ABSTRACT: We have prepared the chiral main-chain LC homopolymer and copolymers which are constructed from the *p,p′*-biphenyldicarboxylic acid as a mesogen component and a certain mixture of chiral (*S*)-2-methylbutanediol and hexanediol as spacer components. These polymers exhibit polymorphism including the chiral nematic, smectic A, and chiral smectic C phases. We have examined the transition behavior between these mesophases and also described the mesophase structure and properties, especially focusing on the ferroelectric chiral smectic C phase.

1. Introduction

The main-chain type of liquid crystal polymers can be characterized by having the mesogen and flexible spacer groups in an alternate fashion.[1] In this type of polymer, the flexible spacer plays a significant role in the mesophase formation since it promotes the orientational and positional arrangements of mesogenic groups which are compatible with the structure of a particular mesophase.

Effects of the flexible spacer on mesophase formation have been extensively studied for the typical main-chain polymers, BB-*n*,[2,3] which tend to form smectic mesophases. One of the most significant effects is derived

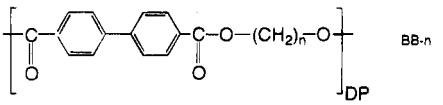

from the fact that two types of smectic structures can be formed depending on an odd–even parity of the carbon number in the alkylene spacer. Through careful identification, it has been found that the polyesters with an even carbon number for the spacer form a smectic A while ones with an odd carbon number form a distinct type of smectic phase, the smectic CA.[3,4] This effect, so-called the even–odd effect, has been understood to result from the conformational constraint in which an angular displacement of neighboring mesogenic groups is strongly confined by a conformation of the flexible spacer.[4]

A second interesting effect is based on the branched spacers and has been studied by treating the following series of homologues:

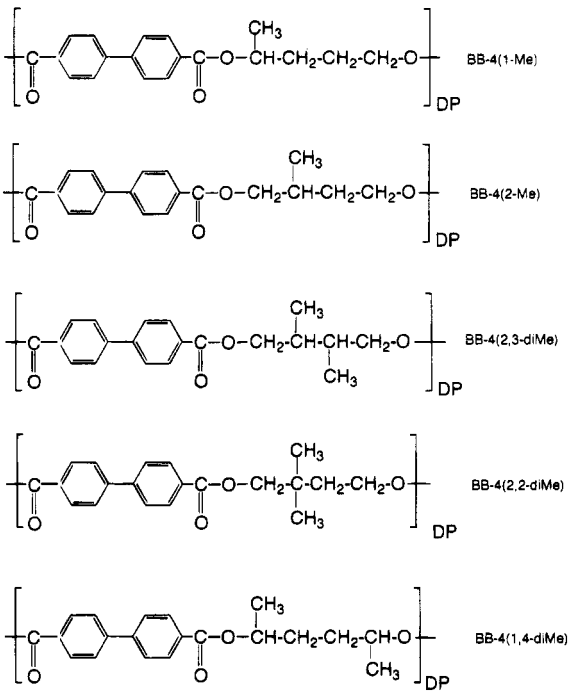

in which one or two branched methyl groups are introduced to the butylene spacer of the BB-4 polyester.[5,6] What is found here is that the mesophase structure is significantly affected by the branched groups. The introduction of one methyl group alters the smectic A of BB-4 to the smectic C phase. Further, branching of two methyl groups tends to collapse the smectic layer structure and in place induces a nematic liquid crystal. This effect has been considered to arise from a steric hindrance of the branched methyl groups.[6]

The second effect is very interesting and encourages us to study the most fantastic mesophase, the chiral smectic C phase, since the asymmetric carbon can be attached to the spacer by branching of a methyl group. The accessible chiral diol as a spacer is (*S*)-2-methylbutanediol and the following main-chain types of BB-*n*

[⊗] Abstract published in *Advance ACS Abstracts,* October 15, 1995.

0024-9297/95/2228-8073$09.00/0

Table 1. Characterization of Polymers

	inherent viscosity (η_{inh}),[b] dL/g	calorimetric data: heating (°C) T_1	T_2	T_i	cooling (°C) T_1	T_2	T_i	kcal/mol ΔH_1[a]	ΔH_2[a]	ΔH_i[a]
BB-4*(2-Me)	0.58		213	234	157	197	224	0.6	0.2	1.4
BB-4*/6(90/10)	0.48		205	231	144	184	222	0.4	0.1	1.4
BB-4*/6(75/25)	0.38	136	184	230	59	181	220	<0.1	0.1	1.5
BB-4*/6(70/30)	0.32	n.s.[c]	178	226	n.s.[c]	175	215	n.s.[c]	<0.1	1.7
BB-4*/6(50/50)-I	0.21	125	175	207	70	172	195	0.3	<0.1	1.7
BB-4*/6(50/50)-II	0.42	130	184	233	73	182	223	0.2	<0.1	1.8
BB-4*/6(50/50)-III	0.98	140	189	241	80	187	230	0.3	0.1	1.9
BB-4*/6(25/75)	0.45		181	238	117	164	223	0.5	<0.1	1.9
BB-4*/6(10/90)	0.33		200	224	131	n.s.[c]	213	0.9	n.s.[c]	2.0
BB-6	0.48		213	239		169	229		1.5	2.3

[a] Based on the cooling DSC data. [b] Measured at 30 °C by using 0.5 g/dL solutions in a 60/40 w/w mixture of phenol and tetrachloroethane. [c] Negligibly small.

homopolymer and copolymers based on this have been prepared in this study:

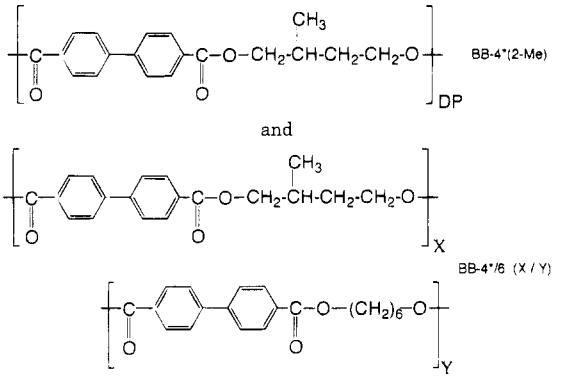

The homopolymer, abbreviated here BB-4*(2-Me), includes a (*S*)-2-methylbutylene spacer, and the copolymers, BB-4*/6(*X*/*Y*), contain (*S*)-2-methylbutylene and hexylene spacers in a certain ratio of *X*/*Y*. The combination of a BB-4*(2-Me) unit with a BB-6 unit in copolymers has been selected for the reason that the homopolymers composed of each unit exhibit similar isotropization temperatures. These polymers form the chiral smectic C and chiral nematic phases as well as the well-known smectic A phase. Their detailed identification and the characteristics in transition behavior between the mesophases are presented in this study. Moreover, we describe the detailed structure and properties of the chiral smectic C phase on the basis of the observations of the X-ray diffraction pattern, light reflection property, and ferroelectric property.

2. Experimental Section

2.1. Materials. Polymers were prepared by melt condensation of *p*,*p*′-biphenyldicarboxylate and an appropriate mixture of (*S*)-2-methylbutanediol and hexanediol. Here, the dimethyl *p*,*p*′-biphenyldicarboxylate and hexanediol were used as received from Tokyo Kasei Kougyo Co., Ltd. The chiral (*S*)-2-methylbutanediol (optical purity; 86%) was kindly supplied by Nippon Oil Co., Ltd. The details of the polymerization procedure have been reported earlier.[2]

The polymers were prepared with inherent viscosities in the range 0.3−0.6 dL/g. The equimolar copolymers were additionally prepared with various inherent viscosities. The characteristics of these polymers, the inherent viscosity, transition temperature, and enthalpy are represented in Table 1.

2.2. Methods. The calorimetric behavior was investigated with a Perkin-Elmer DSC-II calorimeter at a scanning rate of 10 °C/min. The mesophase textures were studied using a polarizing microscope (an Olympus BH-2) equipped with a Mettler FP-80 hot stage. X-ray diffraction photographs were taken at different temperatures by using Ni-filtered Cu Kα radiation. The temperature was measured and regulated by using a Mettler FP-80 heater. The film to specimen distance was determined by calibration with silicon powder. The reflection spectra of the light were measured with Jasco Model J-20 and Hitachi Model 330 spectrometers.

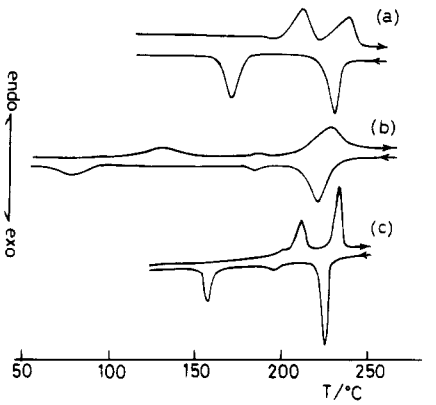

Figure 1. DSC thermograms of (a) BB-6, (b) BB-4*/6(50/50)-II, and (c) BB-4*(2-Me).

The ferroelectric properties of the chiral smectic C phase were investigated by applying a triangular wave voltage which induces the molecules to switch between their two tilted positions. For this investigation, we used a functional generator FS 2201, combined with an amplifier Krohn-Hite 7500 and a storage oscilloscope HP 54503A. The sample was placed between two parallel glass plates coated with a conducting inner surface and separated by spacers of 10−20 μm, with the long axes of molecules homogeneously aligned parallel to the surface.

3. Results

3.1. Transition Behavior of Polymers. 3.1.1. BB-6 Homopolyester. The curves in Figure 1a show the DSC thermograms of BB-6. Two transitions can be well-defined. The mesophase placed between these transitions is a smectic A (S_A), which has been identified in the previous studies.[2,3]

3.1.2. BB-4*(2-Me) Homopolyester. BB-4*(2-Me) undergoes the transition from crystal to chiral nematic (N*) phase at 213 °C on heating (Figure 1c). The isotropization of the N* phase takes place at 234 °C. On cooling, the N* phase and subsequently the chiral smectic C (S_C*) phase are observed. Hence, the S_C* phase is monotropic, appearing from 197 to 157 °C only on cooling.

3.1.3. BB-4*/6*(*X*/*Y*) Copolyesters. Typical DSC thermograms are given in Figure 1b for the equimolar copolymer, BB-4*/6(50/50)-II. Three transitions are well observed. All other copolymers also show two or three

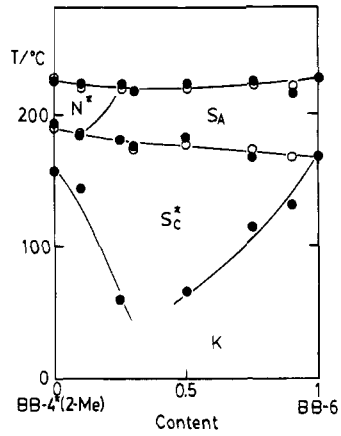

Figure 2. Transition temperatures and phase behaviors of BB-4*/6 copolymers. The transition temperatures given by the closed and open circles were determined from the cooling DSC and microscopic observations, respectively.

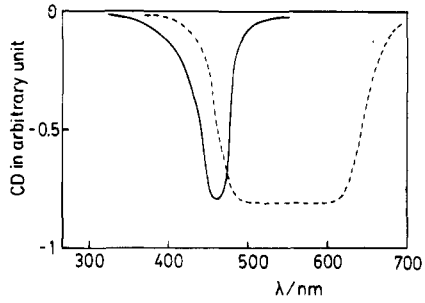

Figure 3. Light reflection bands due to the helical structures as observed by the circular dichroic measurements. The dashed and solid curves were measured for the grandjean aligned N* phase of BB-4*/6(90/10) and the homeotropically aligned S_C* phase of BB-4*/6(75/25), respectively, with the incidence parallel to the helix axis.

transitions on the heating and cooling DSC thermograms. The thermodynamic data are listed in Table 1. The transition temperatures determined from the cooling DSC data are plotted as closed circles against the content of the BB-6 unit in Figure 2. Figure 2 also includes the transition temperatures (open circles) determined from microscopic observations of the textures which will be described later. The transition temperatures by both methods are found to be in a good correspondence and can be smoothly connected so that the phase boundaries are well-defined, as given by the solid curves.

According to Figure 2, the N* phase observed in BB-4*(2-Me) disappears by the introduction of a small content of the BB-6 unit and in place the S_A phase spreads as the highest temperature mesophase over the copolymer region above 25% BB-6 content. Further, the chiral S_C* phase, the lowest temperature mesophase, is formed in the wide temperature region as a result of eutectic-like depression of crystal melting. Thus, the copolymers with BB-6 contents below 25% show the polymorphism in a sequence of K–S_C*–N*–I while those with the contents above 25% exhibit a sequence of K–S_C*–S_A–I.

3.2. Structural Characteristics of the Mesophases. 3.2.1. Chiral Nematic (N*) Phase. The N* phase is easily identified from the observation of grandjean texture, which exhibits visual reflection colors. Its helical structure was examined from the spectroscopic observations of the reflection bands. Figure 3 shows the typical circular dichroic (CD) reflection band observed

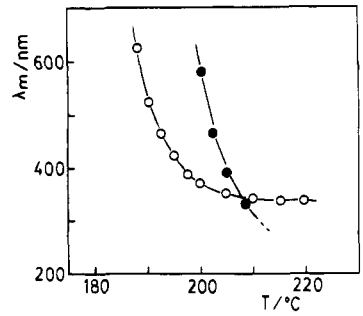

Figure 4. Temperature dependence of the optical pitches (λ_m) in the N* phase (○) for BB-4*/6(90/10) and (●) for BB-4*(2-Me).

for the grandjean-aligned N* phase of BB-4*/6(90/10). The negative sign of the CD band shows that the helical sense of the macrohelix is right-handed. The optical pitches of the macrohelix, the maximum wavelengths of the reflection bands (λ_m), are plotted against the temperature in Figure 4. It can be found that the pitch is less dependent on the temperature although it increases abruptly as the temperature drops to the S_C*–N* transition point.

In Figure 4, the optical pitches for the N* phase of BB-4*(2-Me) are also plotted. Although there is limited observation by spectroscopy, BB-4*(2-Me) shows a temperature dependence similar to that in BB-4*/6(90/10) except for having a relatively small value of pitch.

3.2.2. Smectic A (S_A) Phase. The S_A phase can be identified from the microscopic fan-shape texture (see Figure 5a) and also from the X-ray pattern of oriented specimens (refer to Figure 1 of ref 3). As far as being identified by these methods, the well-defined S_A structure forms invariably from the copolymers. This indicates that the smectic mesophase is able to accommodate considerable disorder in the chemical repeat due to the copolymerization.

The layer spacings elucidated from X-ray diffraction are plotted against the copolymer content in Figure 6. An interesting aspect observed here is that the spacing of layer reflection does not change linearly with the copolymer content; the observed spacing is larger than the averaged value. This unusual variation of layer spacing has been commonly observed in other copolymeric systems,[7] but at this stage it cannot be satisfactorily explained.

3.2.3. Chiral Smectic C (S_C*) Phase. In microscopic observations, the S_C* phase appears as a sanded texture on cooling from the N* phase, while it exhibits a broken fan-shape texture on appearing from the S_A (see Figure 5b). Thus, the transitions between the mesophases can be easily detected by microscopy. The DSC thermograms also show the corresponding transitions: the transition from N* to S_C* takes place as a weak first-order transition (see Figure 1c) while the S_A to S_C* transition is weak first-order or second-order (Figure 1b).

At first, we focus on the layer structure of the S_C* phase, which was analyzed from the X-ray diffraction method by using the equimolar copolymer with the highest molecular weight, BB-4*/6(50/50)-III. This copolymer exhibits the transition from S_A to S_C* at 187 °C, as seen from Table 1. Figure 7a shows the temperature dependence of the spacing of layer reflection. In the S_A phase, layer spacing is nearly constant with a variation of temperature, while on cooling to the S_C* phase, it decreases continuously with decreasing tem-

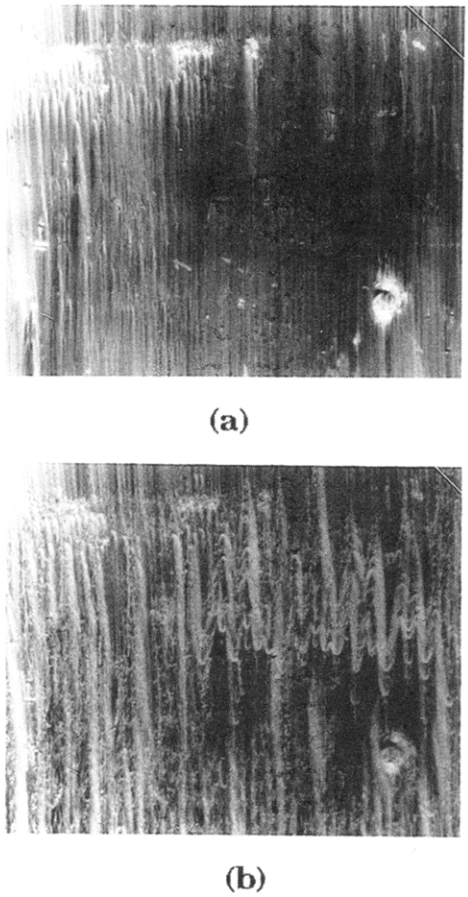

Figure 5. Microscopic textures of the smectic phases of BB-4*/6(50/50)-II. The fan-shape texture of the S_A phase in (a) is altered to the broken fan-shape texture in (b) on cooling to the S_C* phase.

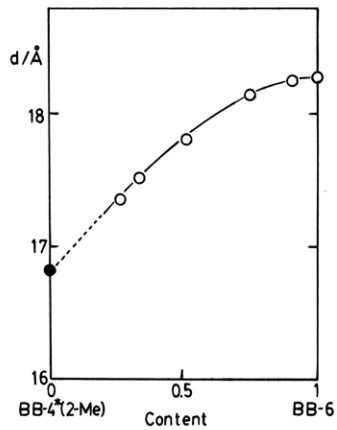

Figure 6. Variation of the layer spacings in the S_A phases with the copolymer content. The closed circle in BB-4*(2-Me) is the tentative value which was evaluated from the layer spacing and the tilt angle of the S_C* phase (refer to the text).

perature. This variation of the layer spacing with temperature is completely reversible on heating and cooling cycles, confirming the formation of the S_C phase with the tilted association of the mesogenic groups with the layer normal.

Tilt angles, θ, can be calculated from the reduction of layer spacing under the assumption that the averaged conformation of polymer chain[5] remains unchanged on phase transition from S_A to S_C* and are plotted against temperature in Figure 7b. One can observe a familiar trend that the tilt angle, θ, increases markedly with the decreasing temperature. Its temperature dependence

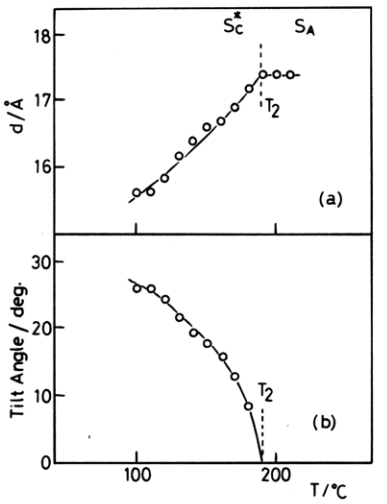

Figure 7. Temperature dependence of (a) the smectic layer spacings and (b) the tilt angles observed for BB-4*/6(50/50)-III. In (b), the tilt angles were calculated from the layer spacing under the assumption that the averaged conformation of polymer chain remains unchanged on phase transition from S_A to S_C*.

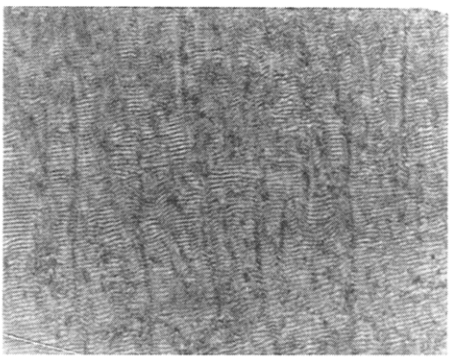

Figure 8. Microscopic texture for the homogeneously aligned S_C* phase of BB-4*/6(10/90). The dechiralization lines attributable to the helical twisting can be observed. The distance between lines is approximately 3 μm.

is expressed by the equation

$$\theta = 2.85(T_2 - T)^{0.46} \text{ (deg)}$$

$$T_2 = \text{transition temperature of } S_C^* \text{ to } S_A$$

which is identical to that observed in the low molar mass S_C* phases.[8] Similar temperature dependence is observed for the other copolymers.

The S_C* phase can also be characterized from the observations of helical structure which is produced by the twist of *c*-directors. Figure 8 indicates the homogeneous texture of the chiral S_C* phase observed in the copolymers with a BB-4*(2-Me) content of 10%. The dechiralization lines attributable to the helical twisting are well observed. Furthermore, when the S_C* is homeotropically aligned, the copolymers with the larger chiral content show the selective reflection of visual light. Shown in Figure 3 is the reflection band detected from the CD measurement. The negative sign of the CD spectrum indicates the right-handed helix.

For all the specimens, the helical pitch was found to be less dependent on the temperature. In Figure 9, the reciprocal pitches elucidated are plotted against the content of the BB-6 unit. Here the closed circles were obtained from the microscopic observation and the open ones from the spectroscopic observation of reflection

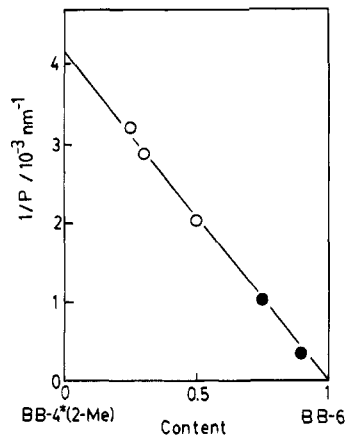

Figure 9. Variation of the reciprocal pitches of the chiral S_C* helix with the content of the BB-6 unit. The closed circles were collected from the microscopic observation of the dechiralization lines (see Figure 8) and the open circles were obtained from the maximum wavelength of the light reflection band (see Figure 3) by assuming the refractive index of 1.4.

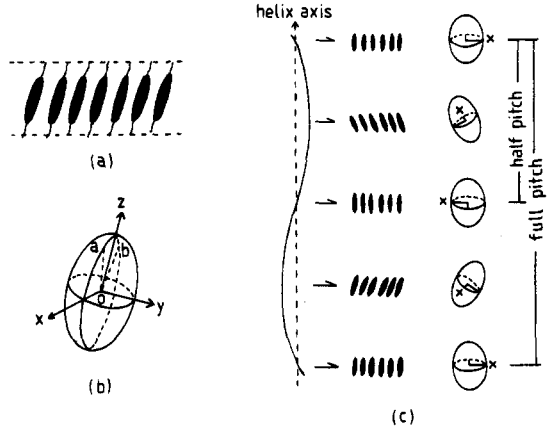

Figure 10. Schematics of (a) molecular ordering in the S_C layer and (b) its optical index ellipsoid. (c) illustrates the helical arrangement of the index ellipsoids in the chiral S_C* phase.

bands. It can be found that the reciprocal pitch (proportional to the twist angle) increases linearly with an increase of the chiral content of the BB-4*(2-Me) unit ($C = X/(X + Y)$) according to the equation

$$1/P = 4.2 \times 10^{-3} C \ (\mathrm{nm}^{-1})$$

It is important to state the interesting aspect with respect to the light reflection properties of the helical S_C* phase. This is derived from the fact that the basic structure of each layer is optically biaxial (see Figure 10a) and that its optical index ellipsoid is tilted to the layer normal. The ellipsoid is illustrated in Figure 10b. Here, the optic plane corresponds to the *xz* plane which is tilted to the layer normal with its plane perpendicular to the tilt direction. The optic axes O*a* and O*b* lie symmetrically on both sides of the O*z* axis. In the chiral S_C* phase, the helix is formed perpendicular to the layer normal so that the index ellipsoids from layer to layer rotate around the axis of the macrohelix with a certain tilting of the O*z* axis. This situation is illustrated in Figure 10c. Because of this characteristic assembly, the selective reflection property of the light strongly depends on the irradiation angle of the light to the helix axis.[9-11] When the light propagates parallel to the helix axis, the selective reflection takes place with the wavelength equal to a half-pitch since the equivalent layer giving

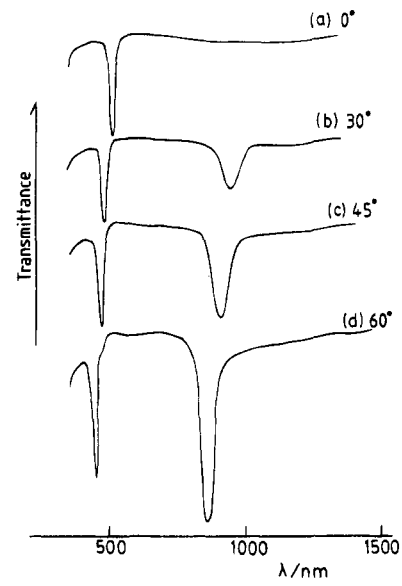

Figure 11. Reflection spectra for the chiral S_C* phase with a homeotropic grandjean alignment which was formed from BB-4*/6(70/30). The reflection spectrum in (a) was measured with the incident light parallel to the helical axis while those in (b)–(d) were measured with incidence inclined by 30, 45, and 60°, respectively.

the same refractive indices appears in every half-pitch of helix. Such a reflection band is called a half-pitch band. In contrast, when the light propagates in a tilted direction to the helix axis, the layer with the same refractive indices no longer appears in every half-pitch but in every full pitch so that a full pitch band should be newly induced at the wavelength position equal to a full pitch. This refractive property is completely different from that of the chiral nematic or chiral S_{CA}* phase[4,9] which exhibits only a half-pitch band even if the irradiation angle of the light is altered.

To confirm this peculiar optical property, the reflection spectra were observed for the homeotropically aligned S_C* phase of BB-4*/6(70/30) which was prepared by strong shearing between glass plates and subsequently glassified by quenching into ice water. The reflection spectra are shown in Figure 11. On the irradiation of the light parallel to the helix axis, only a half-pitch band can be observed (see curve a of Figure 11). On the tilted irradiation the full pitch band appears, its intensity increasing as the irradiation angle is increased (see curves b–d of Figure 11). The results completely correspond to those expected, offering the first distinct example of the light reflection property due to a helical structure of the chiral S_C* phase.

Finally, we refer to the ferroelectric property of the polymeric S_C* phase. In the polymeric system, the mesogenic groups are packed into each layer with a C_2 symmetry, as in the low molar mass system,[12] although the mesogenic groups comprising the layer are linked to each other. In this sense, the ferroelectricity would be reasonably expected.

Ferroelectricity of the present polymeric S_C* phase was simply clarified from the microscopic observation of the elimination of helical structure which takes place on applying the electric voltage. For this observation, the equimolar copolymer with the lowest molecular weight, BB-4*/6(50/50)-I, was used and its homogeneous S_C* was prepared by a weak shearing between glasses coated with a conducting inner surface. Such a homogeneous specimen displays the extinction of the bire-

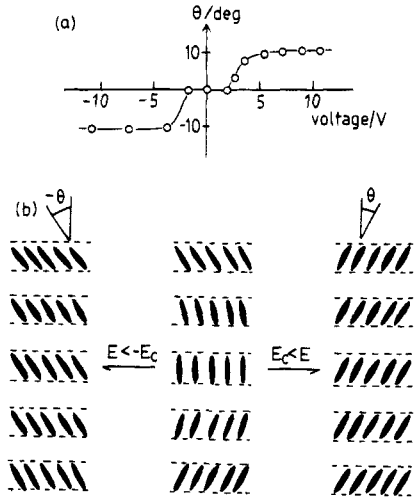

Figure 12. Dependence of rotation angle, θ, on the driving voltage as detected from the microscopic observations of the molecular ordering. The specimen employed here is the homogeneous S_C^* phase of BB-4*/6(50/50)-I, which displays extinction under crossed polarizers when the helical axis is parallel to the polarizer or analyzer plane. When the external voltage is driven above the critical value, the helical structure disappears, as illustrated in (b), and so the extinction is shifted to a new position which can be detected by a rotation of the same stage. The rotation angle, θ, is defined as an angular displacement of the sample stage from its initial position.

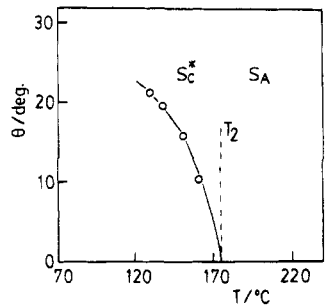

Figure 13. Temperature dependence of the rotation angle, θ, which was determined for BB-4*/6(50/50)-I by the method described in Figure 12.

fringence under crossed polarizers when the helical axis is parallel to the polarizer or analyzer plane. On driving the voltage above the critical value, the characteristic texture due to the helical structure disappears and at the same time the extinction is shifted to a new position which can be detected by a rotation of the sample stage. In Figure 12a is shown the voltage dependence of the rotation angle. One can find that the angle increases from 0° to a certain constant value when the voltage above the critical value is applied. This phenomenon can be explained as a ferroelectric response, and the corresponding structure change is illustrated in Figure 12b where the orientation of layers is maintained but the mesogenic groups reorient unidirectionally in a tilted direction to the layer as a result of untwisting. The rotation angles thus give the tilt angles of the molecule to the layer normal and are plotted against the temperature in Figure 13. It can be found that the temperature dependence is entirely consistent with that elucidated from the X-ray observation (refer to Figure 7b).

Spontaneous polarization, Ps, was determined from the switching current which can be measured by applying a triangular wave voltage with a frequency of 1.1 Hz and an amplitude of 100 V_{p-p}. The experimental data of switching current peak are given in Figure 14a.

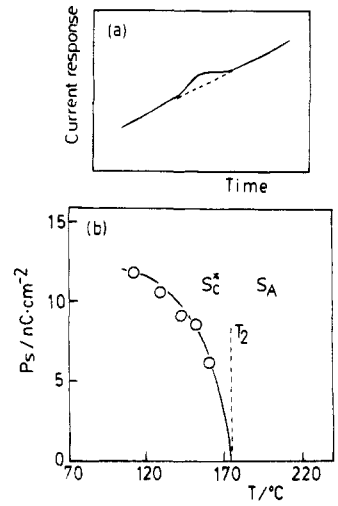

Figure 14. (a) Current response of the S_C^* phase which was driven by a triangular wave voltage with an amplitude of 100 V_{p-p} and a frequency of 1.1 Hz and (b) the temperature dependence of the spontaneous polarization, Ps. The sample employed here is BB-4*/6(50/50)-I.

The values of Ps thus evaluated are plotted against temperature in Figure 14b. There can be seen a temperature variation similar to that in the chiral S_C^* of the conventional monomeric materials; the ferroelectric property arises on the transition from S_A to S_C^*, and the value of Ps increases with decreasing temperature. The maximum value of Ps is around 12 nC/cm^2.

4. Discussion

Firstly, we consider the effects of the branched spacer on the smectic mesophase behavior. These can be extracted by comparing the data from BB-4*(2-Me) and BB-4 which have the same carbon numbers in the spacer directly linking the mesogenic cores. The phase behavior and the transition temperatures observed on cooling these polymers are given below.

$$K \xleftarrow{157\ ^\circ C} S_C^* \xleftarrow{197\ ^\circ C} N^* \xleftarrow{224\ ^\circ C} I \quad \text{for BB-4*(2-Me)}$$

$$K \xleftarrow{251\ ^\circ C} S_A \xleftarrow{298\ ^\circ C} I \quad \text{for BB-4}$$

By this comparison, two significant effects due to the branched methyl group can be recognized. One is observed in the mesophase temperature region; it significantly falls by branching the methyl group, which may be attributable to the reduction in the lateral packing interaction of polymer chains. The second effect can be seen on the type of liquid crystals. Branching of the methyl group alters the smectic A phase to the tilted smectic C phase. Furthermore, it tends to decrease the thermal stability of the smectic phase and newly induces the nematic liquid crystal.

Among these effects, the alteration of S_A to S_C is especially interesting. Considering that a similar alteration can be observed for the other types of polyesters with the branched spacers,[6] this can be simply explained as resulting from the steric hindrance such that the more effective accommodation of branched methyl group into the space between biphenyl layers may be achieved by a tilted association of polymer chains or biphenyl groups.

The BB-4*/6 copolymers showed the following polymorphisms with a different sequence:

$$K - S_C^* - N^* - I$$

for BB-4*/6(X/Y) with X above 75%

$$K - S_C^* - S_A - I$$

for BB-4*/6(X/Y) with X below 75%

which allowed us to examine the detailed structural change on the transition between the phases. We found that the helical pitches of the chiral N* phase diverge near the transition to the smectic mesophase. Further, the tilt angle of the mesogenic groups in the S_C^* phase was observed to decrease in a continuous way with the increasing temperature and finally reach zero in the S_A phase. These phenomena, so called the critical phenomena, are similar to those observed in the monomeric materials.[13] It is thus concluded that the linkage of the mesogenic groups into a polymer does not significantly affect the critical phenomena.

A significant difference between the polymers and monomeric materials may appear with respect to the helical structure of the chiral S_C^* phase. In the monomeric system, the layers are constructed by the individual molecule and its helical structure is formed by the intermolecular twisting. In the polymeric system, on the other hand, the mesogenic groups participating to form a layer are linked to each other through the polymer chain. This leads to the peculiar situation that the polymer molecule itself should also be forced to assume the helical conformation. From the structural parameters observed for the chiral S_C^* phase of the equimolar copolymer, for example the tilt angle of 25°, the layer thickness of 16 Å, and helical pitch of 5000 Å, we can illustrate the helical conformation of polymer with a pitch of 5000 Å and a radius of around 300 Å (refer to Figure 10c). The helix is rather loose and so the polymer chain can approximately be linear at a local portion,[14] but there is no doubt that the polymer chains undergo a certain deformation of bending and twisting.

Considering this particular macrohelix, one may envisage a question of how the helical polymer molecules reorient to the untwisting form as a result of the ferroelectric response on applying the voltage. As far as we are concerned with the microscopic observations in Figure 12, the mechanism for the reorientation of each mesogenic group is apparently similar to that in the monomeric system.[8] In this particular case, however, the polymer chains themselves must reorient. This is hardly practical if the polymer has an appreciably high molecular weight. In fact, the well-defined ferroelectric response can be observed only for the low molecular weight BB-4*/6(50/50)-I, but not for the higher molecular weight homologues. Thus, further investigation is needed to determine precisely the molecular weight of polymers and to clarify the detailed mechanism for the ferroelectric reorientation of polymer molecules.

References and Notes

(1) Ciferri, A., Krigbaum, W. R., Meyer, R. B., Eds. *Polymer Liquid Crystals*; Academic Press: New York, 1982.
(2) Watanabe, J.; Hayashi, M. *Macromolecules* **1988**, *21*, 278.
(3) Watanabe, J.; Hayashi, M. *Macromolecules* **1989**, *22*, 4083.
(4) Watanabe, J.; Kinoshita, S. *J. Phys. II* **1992**, *2*, 1237.
(5) Watanabe, J.; Hayashi, M.; Kinoshita, S.; Niori, T. *Polym. J.* **1992**, *24*, 597.
(6) Watanabe, J.; Tokita, M. To be published.
(7) Watanabe, J.; Krigbaum, W. R. *Macromolecules* **1984**, *17*, 2288.
(8) Beresnev, L. A.; Blinov, L. M.; Osipov, M. A.; Pikin, S. A. *Mol. Cryst. Liq. Cryst.* **1988**, *158A*, 3.
(9) Berreman, D. W. *Mol. Cryst. Liq. Cryst.* **1973**, *22*, 175.
(10) Chilaya, G. S.; Aronishidze, S. N.; Kushnirenko, M. N. *Mol. Cryst. Liq. Cryst. (Lett.)* **1982**, *82*, 281.
(11) Chandani, A. D. L.; Gorecka, E.; Ouchi, Y.; Takezoe, H.; Fukuda, A. *Jpn. J. Appl. Phys.* **1989**, *28*, L-1265.
(12) Meyer, R. B. *Mol. Cryst. Liq. Cryst.* **1977**, *40*, 33.
(13) de Gennes, P. G.; Prost, J. *The Physics of Liquid Crystals*; Oxford University Press: New York, 1993; p 507.
(14) The twist angle of the *c*-director between the successive layers is more or less 1°.

MA950471J